

Metal particle-enhanced fluorescent immunoassays on metal mirrors

Evgenia G. Matveeva^{a,*}, Ignacy Gryczynski^{a,b}, Anne Barnett^{a,c}, Zoya Leonenko^{d,e},
Joseph R. Lakowicz^e, Zygmunt Gryczynski^{a,b}

^a Department of Molecular Biology and Immunology, Health Science Center, University of North Texas, Fort Worth, TX 76107, USA

^b Department of Cell Biology and Genetics, Health Science Center, University of North Texas, Fort Worth, TX 76107, USA

^c Department of Physics, Optical Microcharacterisation Facility, Division of Information and Communication Sciences,
Macquarie University, Sydney, NSW 2109, Australia

^d Department of Cell Biology and Anatomy, Faculty of Medicine, University of Calgary, Calgary, Alberta T2N 4N1, Canada

^e Department of Biochemistry and Molecular Biology, Center for Fluorescence Spectroscopy,
School of Medicine, University of Maryland at Baltimore, Baltimore, MD 21201, USA

Received 2 November 2006

Available online 26 January 2007

Abstract

We present fluoroimmunoassays on plain metal-coated surfaces (metal mirrors) enhanced by metal nanoparticles (silver island films [SIFs]). Metal mirrors (aluminum, gold, or silver protected with a thin silica layer) were coated with SIFs, and an immunoassay (model assay for rabbit immunoglobulin G or myoglobin immunoassay) was performed on this surface using fluorescently labeled antibodies. Our results showed that SIFs alone (on glass surface not coated with metal) enhance the immunoassay signal approximately 3- to 10-fold. Using a metal mirror instead of glass as support for SIFs results in up to 50-fold signal enhancement.

© 2007 Elsevier Inc. All rights reserved.

Keywords: Fluorescence immunoassay; Metal-enhanced fluorescence; Plasmonics; Nano-size metal particles; Silver island films

The interaction of light with small, sub-wavelength-size silver particles results in a significant enhancement of the local electromagnetic field. A recent example of this is surface-enhanced Raman spectroscopy [1–3], where enhanced local field effects have resulted in detection of signal from single molecules [4,5].

In the work presented here, fluorophore molecules located near the silver nanoparticles are exposed to the enhanced local field and are strongly excited. In addition, the excited fluorophores interact with the silver nanoparticles (with localized surface plasmons), resulting in more effective radiation of the excitation energy (fluorescence). This effect is known as radiative decay engineering [6–11]. In general, the fluorescence intensity increase due to the presence of silver nanoparticles can be described as

$$G \sim G_{\text{ex}} G_{\text{qy}}, \quad (1)$$

where G_{ex} describes higher excitation rate due to enhanced local field and $G_{\text{qy}} = Q_{\text{m}}/Q_0$ is the increase in quantum yield of fluorophore near silver island films (SIFs)¹. The contribution of the emission efficiency (increase of the quantum yield) to the total brightness depends on the original quantum yield. It is only approximately 2-fold for the fluorophore with 0.5 quantum yield because the quantum yield cannot exceed 1.0. However, the decrease of the observed lifetime can be significant. For the very high values of the radiative rate, the quantum efficiency approaches 1 and the lifetime is close to zero. The contribution of the enhanced local field to the total brightness can be higher. For example, if the total brightness increases 30-fold, the

* Corresponding author.

E-mail address: ematveev@hsc.unt.edu (E.G. Matveeva).

¹ Abbreviations used: SIF, silver island film; SPR, surface plasmon resonance; anti-Myo, anti-myoglobin; IgG, immunoglobulin G; Myo, myoglobin antigen; AFM, atomic force microscopy.

contribution of the enhanced local field will be responsible for more than 15-fold. At small separation distances of 50 Å or less, fluorophores are strongly quenched by metals.

The effects of silvered nanostructured surfaces on fluorescence from deposited dyes have been studied for a number of years. Various groups have used different methods for metallic surface preparation [12–17] with improvement in the fluorescence brightness up to approximately 20-fold. SIFs and deposited colloids have been used mostly because of ease of preparation procedure and effectiveness. From fluorophores-to-nanostructure distance studies [14,18], it is known that the strongest enhancement occurs at a distance of approximately 100 Å. Surfaces prepared from silver colloids of different size have been tested [19], with the conclusion that the best enhancement is observed for particle clusters. Selective location of the fluorophores on the silver islands gives only a modest improvement in enhancement [20]. Recently reported enhancements from periodic surfaces prepared by electron beam lithography also gave results similar to those obtained on SIFs [21].

Here we present an alternative approach in this quest for strongest fluorescence enhancement. Inspired by reports from the Hayashi group on the effects of metallic particles on the surface plasmon excitation [22,23] and amplification of surface plasmon resonance (SPR) with metallic colloids, as reported by Natan and Lyon [24], as well as earlier work by Aussenegg and coworkers on thin film sensors [25], we studied fluorescence brightness enhancements on SIFs deposited on metallic semitransparent mirrors. We wondered whether highly localized gap modes, observed in SPR experiments in the presence of metallic colloids, will influence the free space brightness of deposited fluorophores.

In this article, we compare the fluorescence brightness observed on bare glass, metallic mirrors, SIFs deposited on glass, and SIFs deposited on metallic mirrors. Two protein systems have been deposited on the surfaces: a model immunoassay with AlexaFluor 555 and a myoglobin immunoassay with AlexaFluor 647.

Materials and methods

Reagents

Rabbit and goat immunoglobulin G (IgG, 95% pure) were obtained from Sigma (USA). AlexaFluor 647-labeled anti-rabbit IgG conjugate and AlexaFluor 555-labeled anti-rabbit IgG conjugate were obtained from Molecular Probes (USA). Buffer components and salts (e.g., bovine serum albumin, glucose, sucrose, AgNO₃) were obtained from Sigma–Aldrich (USA). Myoglobin (recombinant) and monoclonal anti-myoglobin (anti-Myo) antibodies (capture anti-Myo antibodies clone 2 mb-295 and reporter anti-Myo antibodies clone 9 mb-183r) were obtained from Spectral Diagnostics (Canada). Microscope glass slides (3 inches × 1 inch, 1 mm thick) were obtained from VWR Scientific Products (USA). Metal mirror layer was deposited

onto glass microscope slides by EMF (USA). Slides were vapor deposited with continuous 2-nm thick chromium, 48-nm thick gold, and 10-nm thick SiO₂ layers; 50-nm thick silver and 5-nm thick SiO₂ layers; or 50-nm thick aluminum and 5-nm thick SiO₂ layers. Milli-Q purified water was used for all aqueous solutions.

Preparation of mirrors coated with SIFs

For coating with SIFs, we used glass slides coated with a mirror (plain metal layer: 48-nm thick gold, 50-nm thick silver, or 50-nm thick aluminum) and noncoated glass slides as a control. SIF surface was formed according to the procedure described elsewhere [7,26,27]. Briefly, half of the surface of each slide was modified by depositing SIF by chemical reduction of silver nitrate by a wet chemical process using D(+)-glucose. The other half was left unmodified and used as a control.

Model immunoassays

Slides were dried in air and covered with tape containing punched holes (regular-size 6-mm diameter hole puncher) to form wells on the surface of the slides. Model immunoassays were performed on the slide surface in the wells as described previously [26]. Briefly, rabbit IgG was noncovalently immobilized on the sample slide, or goat IgG was noncovalently immobilized on the control slide (slides first were dried with air and covered with tape containing punched holes to form wells). Then AlexaFluor 555-labeled anti-rabbit IgG conjugate was added to the sample slide (with rabbit IgG) or control slide (with goat IgG), and after incubation the fluorescence signal was measured (Fig. 1). A scheme of the model immunoassay is presented in Fig. 2A.

Myoglobin immunoassays

Myoglobin immunoassays were performed in a “sandwich” format (Fig. 2B) as described previously [27]. Briefly, slides (covered with the tape containing punched holes) were noncovalently coated with capture anti-Myo antibody. Then myoglobin antigen (Myo) was added at various concentrations, and after incubation and washing a conjugate of the reporter anti-Myo antibody with AlexaFluor 647 was added, followed by incubation and fluorescence signal measurement. A scheme of the Myo immunoassay is presented in Fig. 2B.

Spectroscopic measurements

Emission spectra in solution were measured using a Varian Cary Eclipse fluorometer (Varian Analytical Instruments, USA). Absorption spectra in solution and on the surface of the slides were measured using a Hewlett–Packard model 8543 spectrophotometer (USA). Fluorescence measurements of the samples on glass slides were performed by placing the slides horizontally on a stage, with

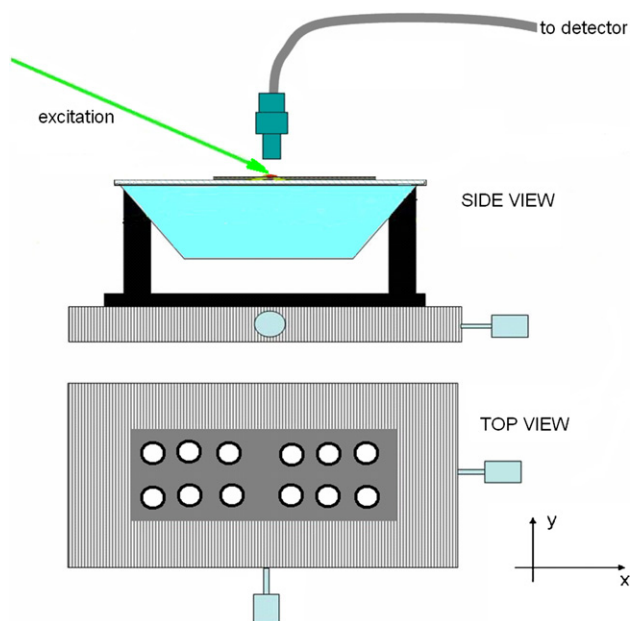


Fig. 1. Experimental setup. The excitation beam (front face) was directed to the slide mounted on the holder movable in the x - y direction, forming an approximately 45° angle with the vertical. Such a configuration allowed easy changes of the slide spot position. The slide was covered with black tape containing holes (12 holes/slide) forming sample wells, similar to a 96-well assay plate. Half of each slide was coated with SIFs (6 wells/slide [SIF coating not shown]). Detection was performed from the top, from the surface inside wells of the slide, by the fiber equipped with the cutoff filter.

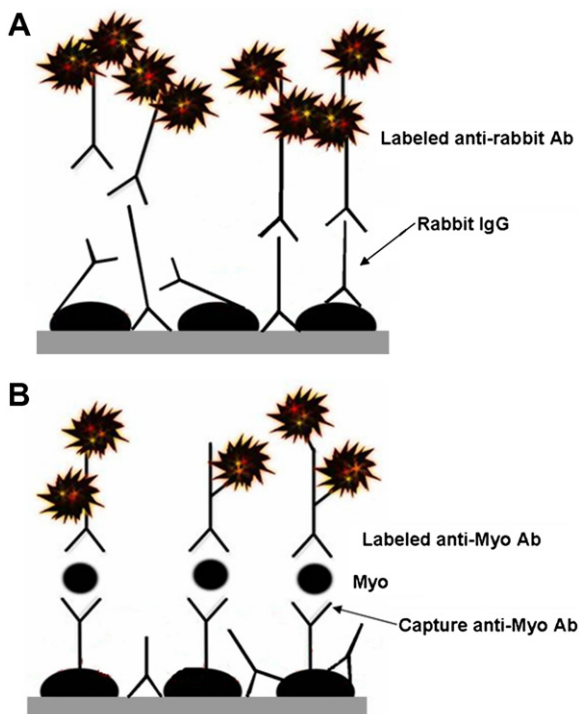


Fig. 2. Scheme of the model immunoassay (A) and myoglobin (sandwich format) immunoassay (B) on the SIF-modified slide surface. Ab, antibody.

excitation at approximately a 45° angle and fluorescence detection from the top of the slide as shown in Fig. 1. For excitation, we used a small solid-state laser with emis-

sion at 532 nm (AlexaFluor 555 or AlexaFluor 647 labels) or a 651-nm emission (AlexaFluor 647 label) laser diode (commercial laser pointer). Emission spectra were collected via a fiber-optic from the top using a Fiber Optics Spectrometer (SD2000, Ocean Optics, USA). For observation, we used appropriate plastic cutoff filters to attenuate excitation lines.

Atomic force microscopy (AFM) images were collected by scanning dry sample slides with an atomic force microscope (TMX 2100 Explorer SPM, Veeco, USA), equipped with an AFM dry scanner, over $100\ \mu\text{m}$. The AFM scanner was calibrated using a standard calibration grid and 100-nm diameter gold nanoparticles from Ted Pella. Images were analyzed using SPMLab software.

Results and discussion

Model immunoassay

We performed the model immunoassay (Fig. 2A, AlexaFluor 555 label) on different substrates (Fig. 3)—gold mirror, silver mirror, and aluminum mirror—as well as on glass only (no metal mirror). Each of these surfaces was either coated or not coated with SIFs. The bare glass substrate served as a reference, and fluorescence signals were referred to the signal obtained from the glass. Then we checked the spectra and backgrounds. Fig. 4 shows the fluorescence spectra of AlexaFluor 555-labeled antibody on the glass and SIF-coated silver, gold, and aluminum mirrors. Spectra were taken after 1 h of incubation of the solution of the labeled antibodies on the antigen-coated surface (and subsequent washing). Our additional experiments on kinetics of binding (not shown) demonstrated that this time period is enough to reach the binding equilibrium ($\sim 95\%$ binding occurs within the first 15 min). We also found that no dissociation of antibodies occurs for at least several days during incubation of the sample with buffer (data not shown). Background signals (not shown) were calculated from fluorescence spectra intensity measurements taken at the same conditions but using the control antigen (goat IgG instead of rabbit IgG). These results reflect the level of nonspecific binding and showed a contribution of 3% or less for all samples.

Fluorescence measurements for each surface were repeated four to six times on different spots (from two or three slides), and the signals were averaged. The results and standard deviations are presented in Table 1. The mirrors without SIFs, as expected, did not enhance fluorescence signals significantly. The fluorescence signals from the immunoassay system on mirrors are approximately twice as strong as those measured from bare glass, a result that can be easily explained by the theory of fluorescence emission near the mirror surfaces [28–34].

The fluorescence signal from SIFs deposited on glass shows an enhancement (the ratio of the peak signal on the SIFs/glass to the peak signal on the bare glass) of 9 to 10. Approximately one order of magnitude fluorescence

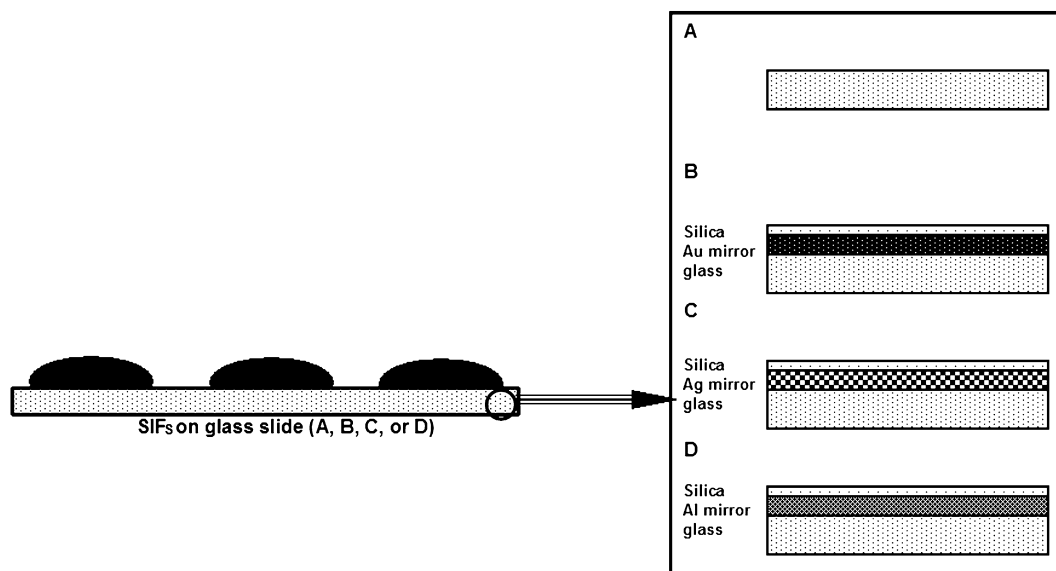


Fig. 3. Scheme of various slide supports used for immunoassay: (A) glass only; (B) glass covered with gold (Au) mirror (48 nm thick) and protecting silica layer (5 nm thick); (C) glass covered with silver (Ag) mirror (50 nm thick) and protecting silica layer (2 nm thick); (D) glass covered with aluminum (Al) mirror (50 nm thick) and protecting silica layer (2 nm thick).

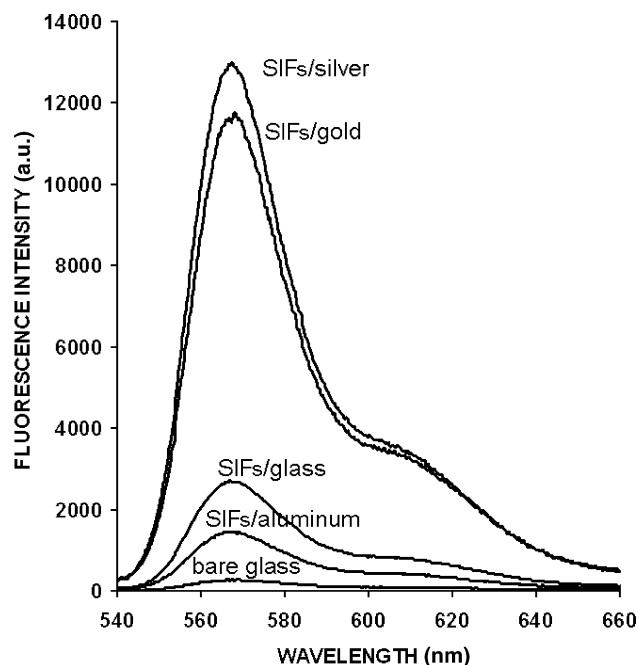


Fig. 4. Fluorescence spectra of the labeled (AlexaFluor 55) anti-rabbit antibodies bound to the antigen immobilized on various slide supports used for immunoassay: glass only, SIFs on aluminum mirror, SIFs on bare glass, SIFs on gold mirror, and SIFs on silver mirror.

enhancements have been reported frequently by various groups. This result is consistent with our previous data [26] and demonstrates that the SIFs and assay have been prepared accurately. Similarly, SIFs were prepared on silver and gold mirrors, and the same model immunoassay has been performed on each slide. In this case, the enhancement of fluorescence signal is much higher (~fivefold) for SIFs deposited on metallic mirrors (Table 1) than for SIFs

deposited on bare glass. We consider this to be a significant improvement in metal-enhanced fluorescence that will allow detection of lower analyte concentrations.

AFM images of the SIF-coated slides are shown in Fig. 5 for the bare glass substrate (top) and gold mirror (bottom). The sizes and densities of the SIFs are similar independent of the substrate. However, sizes and densities vary widely for the same substrate from sample to sample due to manual sample preparation. According to AFM data, the heights of the SIF particles vary from 50 to 150 nm, with an average height of approximately 70 nm. We believe that variations in the fluorescence signal can be partially explained by such inhomogeneity of the particles and can be minimized by improving the method of SIF coating.

Myoglobin immunoassay

We applied the combination of SIFs–metallic mirror substrate to the myoglobin immunoassay using an AlexaFluor 647 label. The fluorescence spectra from the immunoassay performed on bare glass, on SIFs deposited on the bare glass, on SIFs deposited on the gold mirror are shown in Fig. 6. Similar to the model assay, spectra were taken after 1 h of incubation of the labeled antibodies on the antigen-coated surface (and subsequent washing) to reach the binding equilibrium (~95% binding occurs within the first 10–12 min). No dissociation of antibodies occurred for at least several days during incubation of the sample with buffer (data not shown). The signal was linear versus bulk myoglobin concentration within the range of 0 to 300–400 ng/ml (SIF-coated glass [data not shown]), so we chose the myoglobin concentration of 100 ng/ml (which is within the linear range and represents the clinical cutoff) for evaluation of the metal mirror effect. The fluorescence

Table 1

Fluorescence intensities (signal) obtained from the labeled antibodies used in model immunoassay (AlexaFluor 555 label) or in myoglobin immunoassay (AlexaFluor 647 label at 100 ng/ml Myo) from various substrates coated or not coated with SIFs

Substrate	Model immunoassay		Myoglobin immunoassay			
	Signal (at 568 nm)	SD (%)	Excitation 651 nm		Excitation 532 nm	
			Signal (at 670 nm)	SD (%)	Signal (at 670 nm)	SD(%)
Glass	1.0	10.7	1.0	17.9	1.0	11.6
Aluminum	2.6	19.8				
Silver	1.6	15.4	1.1	7.6	1.2	23.3
Gold	2.6	24.6	1.9	11.0	1.8	15.0
SIFs on glass	9.5	4.9	9.9	25.3	7.6	13.1
SIFs on aluminum	5.4	12.7				
SIFs on silver	50.2	14.1				
SIFs on gold	41.4	12.8	50.3	11.0	46.8	16.0

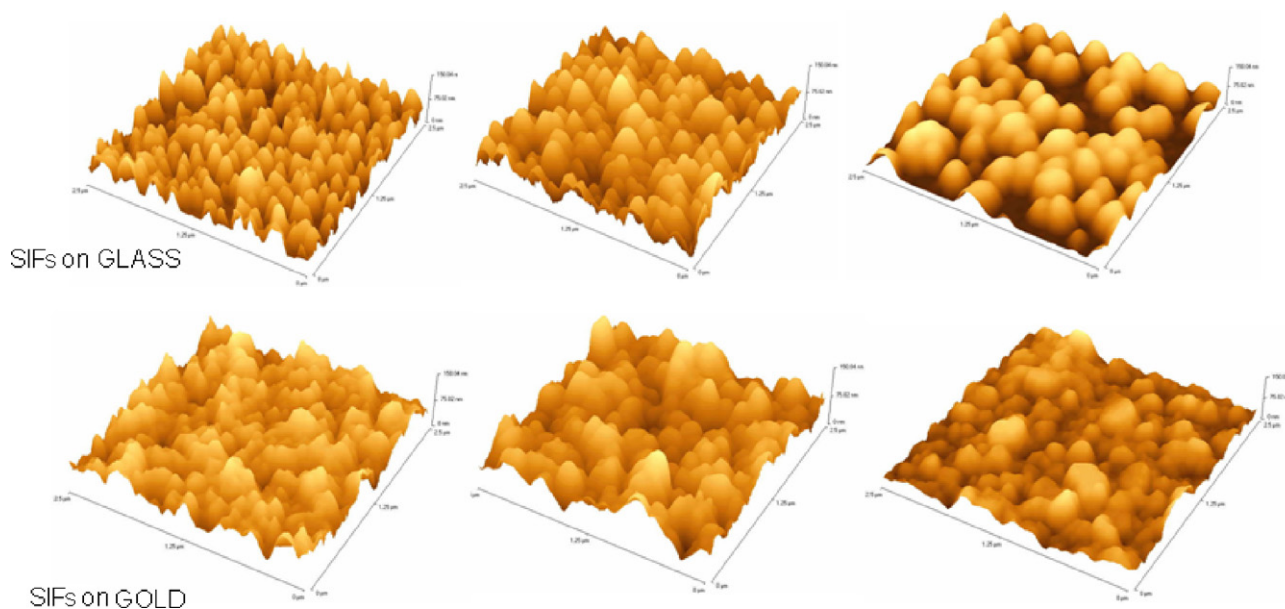


Fig. 5. AFM images of SIF-coated glass (top) and SIF-coated gold mirror (bottom) slides.

intensity from the SIFs–gold mirror system is approximately 8-fold stronger than that from the SIFs–glass system and approximately 50-fold stronger than that from bare glass (Table 1 and Fig. 6). Higher brightness of the dye allows the detection of a lower concentration of myoglobin on SIF-coated mirrors when compared with the noncoated glass surface. It should be noted that the method described is generic and applicable to other markers.

Conclusions

In this work, we presented results showing the high potential of a metal mirror surface modified with SIFs for developing a universal platform for any surface assays by detecting the enhanced fluorescence signal. The results for myoglobin immunoassay and for model immunoassay show that using a mirror layer in combination with SIFs gives approximately 50-fold enhancement compared with approximately 10-fold enhancement when using SIFs without a mirror layer compared with a plain glass substrate.

As outlined in the introductory paragraphs, the enhanced localized electric field associated with small plasmon resonances on metallic nanostructures has been shown to increase the fluorescence lifetime of a fluorophore, resulting in an increased radiative output [6–11]. The system of interest in this work, however, is the extension of the nanoparticle (SIF) supporting glass substrate to one with an underlying metal mirror layer. It has been shown experimentally [35] that systems consisting of nanoparticles with an underlying layer that supports a propagating mode, such as a surface plasmon supporting metallic layer, demonstrate a significant increase in the radiative scattering efficiency when compared with systems where the propagating mode is absent. This increase in radiative scattering efficiency has been attributed to an increase in the dipole–dipole coupling between the localized surface plasmons on the individual nanostructures, mediated by the propagating plasmon mode. The new system studied here takes advantage of not only the increase in fluorescent quantum efficiency associated with the enhanced local fields around the SIF nanostructures but also the highly efficient

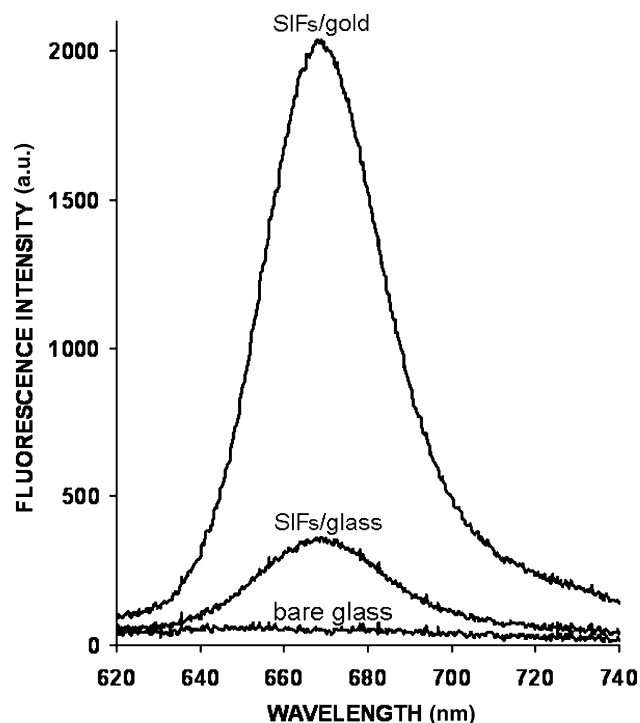


Fig. 6. Fluorescence spectra of the labeled (AlexaFluor 647) reporter anti-Myo antibodies bound to the antigen (myoglobin at 100 ng/ml) immobilized by capture anti-Myo antibodies on various slide supports used for immunoassay: glass only, SIFs on bare glass, and SIFs on gold mirror.

radiative properties of the combined nanoparticle–surface plasmon system. These effects in combination have resulted in the dramatic enhancement in the fluorescence emission from the model and myoglobin immunoassays performed.

Acknowledgments

This research was supported by the National Institutes of Health (NCI CA 114460, NIBIB EB-1690, NCR-08119), BITC, and Philip Morris USA and Philip Morris International.

References

- [1] M. Fleischmann, P.J. Hendra, A.J. McQuillan, Raman spectra of pyridine adsorbed at a silver electrode, *Chem. Phys. Lett.* 26 (1974) 163–166.
- [2] D.L. Jeanmaire, R.P. Van Duyne, Surface Raman spectroelectrochemistry: I. Heterocyclic, aromatic, and aliphatic amines adsorbed on the anodized silver electrode, *J. Electroanal. Chem.* 84 (1977) 1–20.
- [3] K. Kneipp, H. Kneipp, I. Itzkan, R.R. Dasari, M.S. Feld, Surface-enhanced Raman scattering: A new tool for biomedical spectroscopy, *Curr. Sci.* 77 (1999) 915–924.
- [4] S. Nie, S.R. Emory, Probing single molecules and single nanoparticles by surface-enhanced Raman scattering, *Science* 275 (1997) 1102–1106.
- [5] K. Kneipp, H. Kneipp, V.B. Kartha, R. Manoharan, G. Deinum, I. Itzkan, R.R. Dasari, M.S. Feld, Detection and identification of a single DNA base molecule using surface-enhanced Raman scattering (SERS), *Phys. Rev. E* 57 (1998) R6281–R6284.
- [6] J.R. Lakowicz, Radiative decay engineering: Biophysical and biomedical applications, *Anal. Biochem.* 298 (2001) 1–24.

- [7] J.R. Lakowicz, Y. Shen, S. D'Auria, J. Malicka, J. Fang, Z. Gryczynski, I. Gryczynski, Radiative decay engineering: II. effects of silver island films on fluorescence intensity lifetimes and resonance energy transfer, *Anal. Biochem.* 301 (2002) 261–277.
- [8] B.P. Maliwal, J. Malicka, I. Gryczynski, Z. Gryczynski, J.R. Lakowicz, Fluorescence properties of labeled proteins near silver colloid surfaces, *Biopolymers* 70 (2003) 585–594.
- [9] J. Malicka, I. Gryczynski, B.P. Maliwal, J. Fang, J.R. Lakowicz, Fluorescence spectral properties of cyanine dye labeled DNA near metallic silver particles, *Biopolymers* 72 (2003) 96–104.
- [10] A. Parfenov, I. Gryczynski, J. Malicka, C.D. Geddes, J.R. Lakowicz, Enhanced fluorescence from fluorophores on fractal silver surfaces, *J. Phys. Chem. B* 107 (2003) 8829–8833.
- [11] I. Gryczynski, J. Malicka, E. Holder, N. DiCesare, J.R. Lakowicz, Effects of metallic silver particles on the emission properties of $[\text{Ru}(\text{bpy})_3]^{2+}$, *Chem. Phys. Lett.* 372 (2003) 409–414.
- [12] R. Ruppin, Decay of an excited molecule near a small metal sphere, *J. Chem. Phys.* 76 (1982) 1681–1684.
- [13] J. Kummerlen, A. Leitner, H. Brunner, F.R. Aussenegg, A. Wokaun, Enhanced dye fluorescence over silver island films: Analysis of the distance dependence, *Mol. Phys.* 80 (1993) 1031–1046.
- [14] K. Sokolov, G. Chumanov, T.M. Cotton, Enhancement of molecular fluorescence near the surface of metal films, *Anal. Chem.* 70 (1998) 3898–3905.
- [15] P.J. Tarcha, J. DeSaja-Gonzales, S. Rodriguez-Llorente, R. Aroca, Surface-enhanced fluorescence on SiO_2 -coated silver island films, *Appl. Spectrosc.* 53 (1999) 43–48.
- [16] J.R. Lakowicz, J. Malicka, S. D'Auria, I. Gryczynski, Release of the self-quenching of fluorescence near silver metallic surfaces, *Anal. Biochem.* 320 (2003) 13–20.
- [17] C.D. Geddes, A. Parfenov, D. Roll, J. Fang, J.R. Lakowicz, Electrochemical and laser deposition of silver for use in metal-enhanced fluorescence, *Langmuir* 19 (2003) 6236–6241.
- [18] J. Malicka, I. Gryczynski, Z. Gryczynski, J.R. Lakowicz, Effects of fluorophore-to-silver distance on the emission of cyanine dye-labeled oligonucleotides, *Anal. Biochem.* 315 (2003) 57–66.
- [19] J. Lukomska, J. Malicka, I. Gryczynski, J.R. Lakowicz, Fluorescence enhancements on silver colloid coated surfaces, *J. Fluoresc.* 14 (2004) 417–423.
- [20] J. Malicka, I. Gryczynski, J.R. Lakowicz, Fluorescence spectral properties of labeled thiolated oligonucleotides bound to silver particles, *Biopolymers* 74 (2004) 263–271.
- [21] T.D. Corrigan, S. Guo, R.J. Phaneuf, H. Szmanski, Enhanced fluorescence from periodic arrays of silver nanoparticles, *J. Fluoresc.* 15 (2005) 777–784.
- [22] T. Kume, S. Hayashi, K. Yamamoto, A new method of surface plasmon excitation using metallic fine particles, *Mater. Sci. Eng. A* 217/218 (1996) 171–175.
- [23] S. Hayashi, Spectroscopy of gap modes in metal particle–surface systems, *Top. Appl. Phys.* 81 (2001) 71–95.
- [24] M.J. Natan, L.A. Lyon, Surface plasmon resonance biosensing with colloidal Au amplification, in: D.L. Feldheim, C.A. Foss Jr. (Eds.), *Metal Nanoparticles: Synthesis, Characterization, and Applications*, Marcel Dekker, New York, 2002, pp. 183–205.
- [25] F.R. Aussenegg, H. Brunner, A. Leitner, C. Lobmaier, T. Schalkhammer, F. Pittner, The metal island coated swelling polymer over mirror system (MICSPOMS): A new principle for measuring ionic strength, *Sens. Actuat. B* 29 (1995) 204–209.
- [26] E. Matveeva, Z. Gryczynski, J. Malicka, I. Gryczynski, J.R. Lakowicz, Metal-enhanced fluorescence immunoassays using total internal reflection and silver island-coated surfaces, *Anal. Biochem.* 334 (2004) 303–311.
- [27] E. Matveeva, Z. Gryczynski, J.R. Lakowicz, Myoglobin immunoassay based on metal particle-enhanced fluorescence, *J. Immunol. Methods* 302 (2005) 26–35.
- [28] K.H. Drexhage, Influence of a dielectric interface on fluorescence decay time, *J. Luminesc.* 1/2 (1970) 693–701.

- [29] K.H. Drexhage, Interaction of light with monomolecular dye lasers, in: E. Wolf (Ed.), *Progress in Optics XII*, North-Holland, Amsterdam, 1974, pp. 161–232.
- [30] R.R. Chance, A. Prock, R. Silbey, Lifetime of an emitting molecule near a partially reflecting surface, *J. Chem. Phys.* 60 (1974) 2744–2748.
- [31] B.N.J. Persson, Theory of the damping of excited molecules located above a metal surface, *J. Phys. C* 11 (1978) 4251–4269.
- [32] G.W. Ford, W.H. Weber, Electromagnetic effects on a molecule at a metal surface, *Surf. Sci.* 109 (1981) 451–481.
- [33] G.E. Korzeniewski, T. Maniv, H. Metiu, Electrostatics at metal surfaces: IV. The electric fields caused by the polarization of a metal surface by an oscillating dipole, *J. Chem. Phys.* 76 (1982) 1564–1573.
- [34] W.L. Barnes, Fluorescence near interfaces: The role of photonic mode density, *J. Mod. Opt.* 45 (1998) 661–699.
- [35] H.R. Stuart, D.G. Hall, Enhanced dipole–dipole interaction between elementary radiators near a surface, *Phys. Rev. Lett.* 80 (1998) 5663–5666.